

## Influence of atomic relaxations on the structural properties of SiC polytypes from *ab initio* calculations

P. Käckell, B. Wenzien, and F. Bechstedt

*Friedrich-Schiller-Universität, Institut für Festkörpertheorie und Theoretische Optik,  
Max-Wien-Platz 1, 07743 Jena, Germany*

(Received 18 March 1994)

A systematic study of ground-state properties of cubic and hexagonal silicon carbide polytypes (3C-, 6H-, 4H-, and 2H-SiC) is reported using well converged density-functional calculations within the local-density approximation and norm-conserving, fully separable, soft, *ab initio* pseudopotentials. Equilibrium results are obtained for the lattice parameters, atomic positions, bond lengths and angles, cohesive energies, and the bulk modulus. The internal degrees of freedom, i.e., atomic relaxations, are fully taken into account. The results are discussed in comparison with experimental data. We derive trends with the hexagonality for the molecule volume and the energetic ordering of the polytypes. Driving forces for the polytypism and the atomic relaxations are discussed.

### I. INTRODUCTION

Silicon carbide (SiC) is an interesting semiconductor for various electronic, optoelectronic, optical, thermal, and mechanical applications in high-power and high-temperature devices.<sup>1</sup> In addition, SiC is one of the few compounds which form many stable and long-range ordered modifications, the so-called polytypes.<sup>2</sup> Currently, considerable effort is being made to prepare bulk SiC crystals as well as thin layers of different polytypes of good quality. On the other hand, many researchers have refocused their attention to the electrical, optical, elastic, and thermal properties of the material. All these properties depend directly or indirectly via the electronic band structure or the lattice vibrations on the atomic structure of the polytype. There also seems to be an internal relationship between the stability of SiC polytypes and the exact atomic positions, which should be displaced with respect to that of the ideal tetrahedral structure, which is realized, e.g., in the cubic zinc-blende 3C-SiC. These atomic relaxations differ for the various polytypes. They can therefore tell us about the driving forces of the polytypism.

More than a hundred different SiC polytypes are known.<sup>2</sup> However, only for the wurtzite 2H-SiC (Refs. 3 and 4) and another hexagonal modification, 6H-SiC,<sup>5</sup> have careful x-ray measurements of the nonideal bond lengths and angles been done. <sup>29</sup>Si and <sup>13</sup>C NMR studies<sup>6-9</sup> reported the occurrence of different kinds of sites in common polytypes, e.g., 3C, 4H, 6H, and 15R. *Ab initio* pseudopotential calculations are mainly directed to the ground-state properties of the simplest polytypes, the zinc-blende<sup>10-17</sup> and the wurtzite<sup>14,15,17,18</sup> structure. Only in a few cases have polytypes with larger unit cells as 4H, 6H, and 15R been attacked.<sup>14,15</sup> In this context, temperature effects have been also discussed via the free energy of the vibrating lattice.<sup>19</sup> Other density-functional theory (DFT) approaches<sup>20</sup> in

the local-density approximation (LDA),<sup>21</sup> as the linear-muffin-tin orbital (LMTO) method, have only been applied to the elastic properties of 3C-SiC.<sup>22</sup> Within the semiempirical atomic-sphere approximation (ASA) structural properties of 3C- and 2H-SiC (Ref. 23) have also been discussed.

The aim of the calculations<sup>10-18,22,23</sup> was essentially the minimization of the total energy with respect to the lattice constants  $a$  and  $c$  and to find equilibrium values for the characteristic lengths, the bulk modulus  $B$ , and the cohesive energy  $E_{\text{coh}}$ . Most of the calculations for the noncubic polytypes are not complete. Apart from Ref. 15 the internal degrees of freedom, more strictly speaking the atomic relaxations from the "ideal" positions, which are only defined by the two lattice constants, were neglected to minimize the energy. Sometimes,<sup>23</sup> the  $c/a$  ratio is additionally fixed. In the more complete calculations of Cheng, Heine, and Needs<sup>15</sup> the noncubic structures are only relaxed until the Hellmann-Feynman forces<sup>24,25</sup> more or less reach the same values as in the 3C-SiC polytype. In their calculation, this 3C structure is not stress free since the experimental cubic lattice constant  $a_0$  and not the theoretical one is used. In general, reasonable values follow for the lattice constants, even if they are somewhat smaller than the experimental data. However, the volume change, calculated for the 2H polytype with respect to the 3C structure within all DFT-LDA studies,<sup>14,15,17,18,23</sup> is opposite in sign to the reported experimental result.<sup>3</sup>

A second type of contradicting results of the DFT-LDA investigations concerns the energetical order of the polytypes. The LMTO-ASA calculations of Lambrecht and Segall<sup>23</sup> predict the wurtzite structure to be stable with respect to the zinc-blende SiC by about 0.5 eV per SiC molecule. In contrast to this finding the work of Cheng and co-workers<sup>14,15</sup> indicates that the zinc-blende structure is energetically more favorable by  $\sim 10$  meV/mol. Thereby, this result is practically not influenced by the

atomic relaxations. On the one hand, usually structural energy differences of the order of 0.01 eV (or even smaller values) approach the limits of accuracy of the theoretical methods due to different computational details. On the other hand, if they are derived within the same calculational details, they should be accepted to be real differences and discussed in terms of the driving forces of the polytypism. Certainly for finite temperatures the electronic and static-lattice contributions (especially that related to the atomic relaxations) to the polytype stability has to be discussed together with the effect of the free-phonon energy, which should stabilize the polytypism.<sup>19</sup>

In this paper, we report well-converged *ab initio* DFT-LDA calculations of the ground-state properties of the most important hexagonal polytypes, 6H-, 4H-, and 2H-SiC, in comparison to the underlying stress-free zinc-blende 3C-SiC structure. The internal degrees of freedom, i.e., the atomic relaxations, are fully taken into account. We derive results for the lattice constants, atomic positions, cohesive energies, and the bulk modulus. The influence of the atomic relaxations is discussed in more detail. We clarify the energetical ordering of the polytypes at zero temperature as well as the correct trend of the molecule volume with the hexagonality of the structure. The contributions of the electrons and the static ion-ion interaction to the driving forces for the polytypism and the atomic relaxations are discussed. We give bond lengths and bond angles for the stress-free polytypes and explain the trends versus the percentage hexagonality, that are found experimentally.

## II. COMPUTATIONAL ASPECTS

### A. Method of calculation

The parameter-free total-energy, force, and electronic-structure calculations are performed within the DFT.<sup>20,21</sup> The exchange-correlation functional of the many-body electron-electron interaction is approximated by its local version.<sup>21</sup> Explicitly the electron-gas data of Ceperley and Alder<sup>26</sup> are taken into account in the form as parametrized by Perdew and Zunger.<sup>27</sup> The electron-ion interaction is treated using norm conserving,<sup>28</sup> *ab initio*, fully separable pseudopotentials in the Kleinman-Bylander form.<sup>29,30</sup> They are based on relativistic all-electron calculations for the free atom by solving the Dirac equation self-consistently.<sup>28,29</sup>

Within the applied self-consistent method the electronic wave functions are expanded in terms of plane waves. The number of plane waves in such an expansion is determined by the energy cutoff. In the beginning of our studies, the norm-conserving pseudopotentials were generated for Si and C according to the data of Ref. 30, giving rise to potentials similar to those of Bachelet, Hamann, and Schlüter (BHS).<sup>28</sup> Unfortunately, for this choice of the carbon pseudopotentials the energy cutoff should be rather large, about 100 Ry, due to the lack of core *p* states to reach convergence in both the ground state and electronic properties. Therefore, we

use the degrees of freedom that one has in generating such pseudopotentials<sup>17,31</sup> to our advantage by carefully choosing the core radii  $r_c$  for carbon, outside of which true and pseudowave functions are identical.<sup>28-30</sup> Enlarging  $r_c$  means softening of the pseudopotentials, i.e., a smaller number of plane waves is required. In the BHS type potentials,  $r_c$  is determined by a parameter  $cc_l$ ,  $r_c = r_{\max}/cc_l$ , where  $r_{\max}$  is the position of the outermost peak in the all-electron wave function and  $l$  means the quantum number of the angular momentum.

We generate pseudopotentials for angular momentum components  $l = 0, 1$ , and 2. The corresponding parameters are  $cc_s = 1.7$  and  $cc_p = 1.6$ . They are somewhat smaller than the BHS values,  $cc_s = 1.8$  and  $cc_p = 3.0$ . The *d* potential, which plays the role of the local part, has not been modified. For silicon, we use the pseudopotentials given in Ref. 30. In a previous paper,<sup>17</sup> we have clearly shown that the convergence of the physical quantities with the cutoff is much more rapid if the modified carbon pseudopotentials are applied instead of the BHS ones. The energy cutoff can be reduced to a value of about 34 Ry. Nevertheless, we have checked all calculations with a cutoff of 45 Ry. We have found practically no change in the atomic coordinates and the total energy differences between the polytypes. There was only a small rigid shift of the total energies themselves. Similar results of the pseudopotential softening follow for the other first-row elements.<sup>32</sup>

In order to determine the equilibrium atomic positions in the zinc-blende case, only the cubic lattice constant  $a_0$  has to be varied until the total energy reaches the minimum. In the hexagonal cases, we vary the corresponding lattice constant  $a_0 = \sqrt{2}a$  as well as the ratio of the hexagonal lattice constants  $c/a$ . For each considered pair,  $c$  and  $a$ , the positions of the atoms in the unit cell of the crystal are relaxed toward a minimum total energy  $E_{\text{tot}}(c, a)$  and vanishing atomic forces. More in detail, we use a steepest-descent method for the atomic displacements together with a Car-Parrinello-like approach<sup>33</sup> for bringing the wave functions to self-consistency. One important advantage is to avoid the direct diagonalization of the Kohn-Sham equations,<sup>21</sup> which is difficult to handle for the 5400 plane waves taken into account for the 12H structure. In the explicit calculations, we apply the computer code fhi93cp of Stumpf and Scheffler.<sup>34</sup>

Considering the atomic relaxations in the hexagonal cells the equilibrium geometry is identified when all atomic forces are smaller than  $10^{-4}$  a.u., i.e., 0.005 eV/Å. This corresponds to uncertainties in the energies (per pair) of less than 0.001 eV and in the atomic positions of less than 0.002 Å for a given total-energy functional and calculational scheme. Because of the uncertainties, after finding the minimum, we symmetrize the atomic positions in the hexagonal cells to derive a structure in agreement with the  $C_{6v}^4$  space-group symmetry and the fixed hexagonal lattice constants  $c$  and  $a$ .

The accuracy of the determination of the equilibrium constants,  $c$  and  $a$ , and the corresponding total energy  $E_{\text{tot}}$  is higher than that for finding the exact atomic positions within the unit cells. This is reached by a two-dimensional polynomial fit close to the minimum of

$E_{\text{tot}}(c, a)$  taking into account many triplets of numbers  $E_{\text{tot}}$ ,  $c$ , and  $a$ . Usually cubic forms are sufficient. Murnaghan's equation of state<sup>35</sup> cannot be applied to the hexagonal polytypes with sufficient accuracy. Such a fitting procedure has two advantages. First, the effect of the numerical noise due to the finite number of plane waves as well as integration points in the first Brillouin zone is remarkably reduced by the least-square fit. Second, the minimum itself and, hence, the equilibrium values of  $c$ ,  $a$ ,  $E_{\text{tot}}$ , and the second derivative of the energy with respect to the volume, i.e., the bulk modulus  $B$ , are much more accurately determined. From fits to different number of triples close to the minimum we estimate the uncertainties for fixed cutoff and  $\mathbf{k}$  point set to be smaller than  $10^{-4}$  Ry/Si-C pair and  $0.002 \text{ \AA}$  for the lattice constants.

Another problem concerns the estimation of the cohesive energy. The energies of the free Si and C atoms have to be known. The values  $-3.7499$  and  $-5.3334$  a.u. obtained within the described DFT-LDA scheme are too low by about several tenths of an electron volt. Moreover, the experimental total energy of the solids is influenced by the energy due to zero-temperature vibrations of the atoms, which may be estimated to be  $0.01$  a.u./Si-C pair.<sup>11</sup> Both effects lead to an overestimation of the cohesive energy. Such an overestimation of cohesive energies of semiconductors by roughly  $0.5 - 1.5$  eV per atom is well known for the typical DFT-LDA procedures of calculations.<sup>36</sup> Nevertheless, we may use these values since we only compare energy differences between different polytype structures.

One important point of the calculations is the Brillouin-zone integration, appearing in particular in the definitions of the electron density and the kinetic energy. The sampling of the wave functions in  $\mathbf{k}$  space is crucial in achieving the desired accuracy in the total energies. This remains true, although we use partial occupation numbers, according to a Fermi function with an effective electron temperature of  $k_B T = 0.1$  eV, to improve the  $\mathbf{k}$ -space sampling over the Brillouin zone. We apply different techniques in dependence on the consideration of atomic relaxations and the considered quantities, structural parameters, or energies. First, without atomic relaxations the results are obtained involving  $\mathbf{k}$ -space sampling on a regular three-dimensional mesh, which was generated by the method of Monkhorst and Pack.<sup>37</sup> In the irreducible wedge of the Brillouin zone of the polytypes a mesh of 14 points for  $6H$  and  $4H$ , 20 points for  $2H$ , and 10 points for  $3C$  is defined, which is shown to be sufficient for the desired accuracy.<sup>15,16</sup> The energy differences between the polytypes are so small that they can be remarkably influenced by the  $\mathbf{k}$ -point set. Therefore, after finding the equilibrium lattice constants  $a_0$ ,  $c$ , and  $a$  as well as the bulk modulus  $B$ , we repeat the total-energy calculations for fixed lattice constants by describing the  $3C$ -,  $6H$ -,  $4H$ -, and  $2H$ -SiC polytypes within a  $12H$  structure with the corresponding Brillouin zone and 14 special points in the irreducible wedge. Second, in the case with the consideration of the atomic relaxations for a given pair  $c$ ,  $a$  we apply a similar procedure. However, the special  $\mathbf{k}$  points are generated according to Chadi and Cohen<sup>38</sup> using the special scheme of Evarestov and

Smirnov.<sup>39</sup> Because of the symmetry adaption the convergence is improved and the number of special points can be reduced. We apply six mesh points for the hexagonal polytypes. In the worst case,  $2H$ , we have checked the convergence with the number of 3, 6, or 12 special points for fixed ratio  $c/a=1.64$ . We found for the total energies per cell  $E_{\text{tot}}=-19.41191$ ,  $-19.40176$ ,  $-19.40186$  a.u., the lattice constant  $a_0=8.0950$ ,  $8.1020$ ,  $8.1027$  a.u., and for the bulk modulus  $2.35$ ,  $2.25$ ,  $2.26$  Mbar. In order to achieve the accuracy in the energy differences, all structures including the zinc blende one are again specified in terms of  $12H$  hexagonal unit cells and total energies are derived with six Chadi-Cohen points.

## B. Polytype description

The atomic positions  $\mathbf{R}_s = \mathbf{R} + \mathbf{r}_s$  ( $s = 1, \dots, 2p$ ) of the different polytype structures are defined by the Bravais lattice  $\mathbf{R} = \sum_{i=1}^3 n_i \mathbf{a}_i$  ( $n_i$  is an integer) and a certain atomic basis  $\mathbf{r}_s$ , within one unit cell defined by a Bravais lattice vector  $\mathbf{R}$ . The unit-cell vectors of the zinc-blende structure are

$$\begin{aligned} \mathbf{a}_1 &= a_0 \left(0, \frac{1}{2}, \frac{1}{2}\right), \\ \mathbf{a}_2 &= a_0 \left(\frac{1}{2}, 0, \frac{1}{2}\right), \\ \mathbf{a}_3 &= a_0 \left(\frac{1}{2}, \frac{1}{2}, 0\right), \end{aligned} \quad (1)$$

where  $a_0$  is the cubic lattice constant and the Cartesian coordinate system is defined by the cubic axis. There are two atoms per unit cell, Si at  $a_0(0, 0, 0)$  and C at  $a_0(\frac{1}{4}, \frac{1}{4}, \frac{1}{4}) = \frac{1}{4}(\mathbf{a}_1 + \mathbf{a}_2 + \mathbf{a}_3)$ . Here, only the value of  $a_0$  needs to be optimized.

For the hexagonal polytypes or the hexagonal representation of  $3C$ -SiC, the introduction of a Cartesian coordinate system with  $x_{\text{hex}} \parallel [110]$ ,  $y_{\text{hex}} \parallel [11\bar{2}]$ , and  $z_{\text{hex}} \parallel [111]$  is reasonable. The corresponding coordinate transformation is orthogonal. In the Cartesian coordinate system the vectors of the characteristic tetrahedron take the form

$$\begin{aligned} \tau_1 &= \left(0, 0, \frac{3c}{4p}\right), \\ \tau_2 &= \left(\frac{a}{2}, \frac{a}{2\sqrt{3}}, -\frac{1c}{4p}\right), \\ \tau_3 &= \left(-\frac{a}{2}, \frac{a}{2\sqrt{3}}, -\frac{1c}{4p}\right), \\ \tau_4 &= \left(0, -\frac{a}{\sqrt{3}}, -\frac{1c}{4p}\right), \end{aligned} \quad (2)$$

where  $p = 3$  in  $3C$ -SiC and  $p = 6, 4, 2$  in  $pH$ -SiC denotes the number of atomic double layers perpendicular to the hexagonal axis. The primitive lattice vectors could be chosen to be

$$\begin{aligned} \mathbf{a}_1 &= a(1, 0, 0), \\ \mathbf{a}_2 &= a\left(-\frac{1}{2}, \frac{\sqrt{3}}{2}, 0\right), \\ \mathbf{a}_3 &= c(0, 0, 1). \end{aligned} \quad (3)$$

Each SiC double layer consists of two atomic sublayers, one of pure Si and the other of pure C, both in a hexagonal arrangement.

The resulting atomic structures are shown in Fig. 1. The atomic positions  $\mathbf{r}_s$  follow from suitable combinations of the tetrahedron vectors in Eq. (2). In the hexagonal polytypes the atoms of the  $p$  Si-C pairs are all on trigonal axes in special positions in agreement with the  $C_{6v}^4$  ( $P6_3mc$ ) space-group symmetry. The general formation laws are given in the textbook of Wyckhoff<sup>40</sup> or can be taken from the characteristic chain structures within the unit cells represented in Fig. 1. Describing the coordinates in terms of the primitive basis vectors  $\mathbf{a}_i$  ( $i = 1, 2, 3$ ) of Eq. (3) and displacing them eventually by  $\mathbf{a}_1$  or  $\mathbf{a}_2$  toward the coordinate zero the  $2p$  atoms in the unit cell are in the following positions. In the wurtzite ( $2H$ ) structure [cf. Fig. 2(a)] one finds

$$0 \ 0 \ u, \ \frac{1}{3} \ \frac{2}{3} \ \frac{1}{2} + u$$

with  $u(\text{Si})=0$  and  $u(\text{C})=\frac{3}{8}+\epsilon$ , where  $\epsilon$  denotes the dimensionless cell-internal structural parameter. In the case of ideal tetrahedra it holds  $c/a = \sqrt{8/3}$  and  $\epsilon = 0$ . In the  $4H$ ,  $6H$ , and  $3C$  cases the formation laws are [cf. Figs. 2(b) and 2(c)]

$$0 \ 0 \ u, \ \frac{1}{3} \ \frac{2}{3} \ v, \ \frac{2}{3} \ \frac{1}{3} \ w.$$

The atomic positions in the  $4H$  case follow by choosing

$u(\text{Si})=0$ ,  $u(\text{C})=\frac{3}{16}+\epsilon(1)$ ,  $v(\text{Si})=\frac{1}{4}+\delta(2)$  and  $\frac{3}{4}+\delta(2)$ ,  $v(\text{C})=\frac{7}{16}+\epsilon(2)$  and  $\frac{15}{16}+\epsilon(2)$ ,  $w(\text{Si})=\frac{1}{2}$ ,  $w(\text{C})=\frac{11}{16}+\epsilon(1)$ , where  $\epsilon(1)$ ,  $\delta(2)$ , and  $\epsilon(2)$  represent the three small quantities giving the deviations from the positions in the ideal structure, i.e., the structure  $c/(pa)=\sqrt{2/3}$  and  $\epsilon(1) = \delta(2) = \epsilon(2) = 0$ . Without loss of generality  $\delta(1) \equiv 0$  is chosen. For the  $6H$  polytype, one can write  $u(\text{Si})=0$  and  $\frac{1}{2}$ ,  $u(\text{C})=\frac{1}{8}+\epsilon(1)$  and  $\frac{5}{8}+\epsilon(1)$ ,  $v(\text{Si})=\frac{1}{6}+\delta(2)$  and  $\frac{5}{6}+\delta(3)$ ,  $v(\text{C})=\frac{7}{24}+\epsilon(2)$  and  $\frac{23}{24}+\epsilon(3)$ ,  $w(\text{Si})=\frac{1}{3}+\delta(3)$  and  $\frac{2}{3}+\delta(2)$ ,  $w(\text{C})=\frac{11}{24}+\epsilon(3)$  and  $\frac{19}{24}+\epsilon(2)$ , where the five small parameters  $\epsilon(1)$ ,  $\delta(2)$ ,  $\epsilon(2)$ ,  $\delta(3)$ , and  $\epsilon(3)$  are introduced to characterize the atomic relaxations in the system. In the case of the  $3C$  structure all positions are fixed together with  $c/a=\sqrt{6}$ . One has  $u(\text{Si})=0$ ,  $u(\text{C})=\frac{1}{4}$ ,  $v(\text{Si})=\frac{1}{3}$ ,  $v(\text{C})=\frac{7}{12}$ ,  $w(\text{Si})=\frac{2}{3}$ ,  $w(\text{C})=\frac{11}{12}$ .

The atomic positions in the hexagonal polytypes are indicated in more detail in Fig. 2. In this figure the characteristic zig-zag chains are plotted in the  $(11\bar{2}0)$  plane within a rectangular coordinate system spanned by the Bravais-lattice vectors  $-\mathbf{a}_1+\mathbf{a}_2$  and  $\mathbf{a}_3$ . Half of the atoms are labeled by  $X(1)$  to  $X(p/2)$  ( $X=\text{Si,C}$ ), the other half by  $X(1')$  to  $X(p'/2)$ . The prime indicates that the position of these atoms can be described by a displacement of the first ones by a vector  $\frac{p}{6} \frac{p}{6} \frac{1}{2}$  and a subsequent rotation around the  $c$  axis by  $180^\circ$ . In this figure the origin of the stacking sequences of atomic SiC double layers in  $[0001]$  direction is also indicated, following the chain links in the three different  $(11\bar{2}0)$  planes  $A$ ,  $B$ , and  $C$  in a hexagonal unit cell. In addition, the cubic ( $c$ ) or

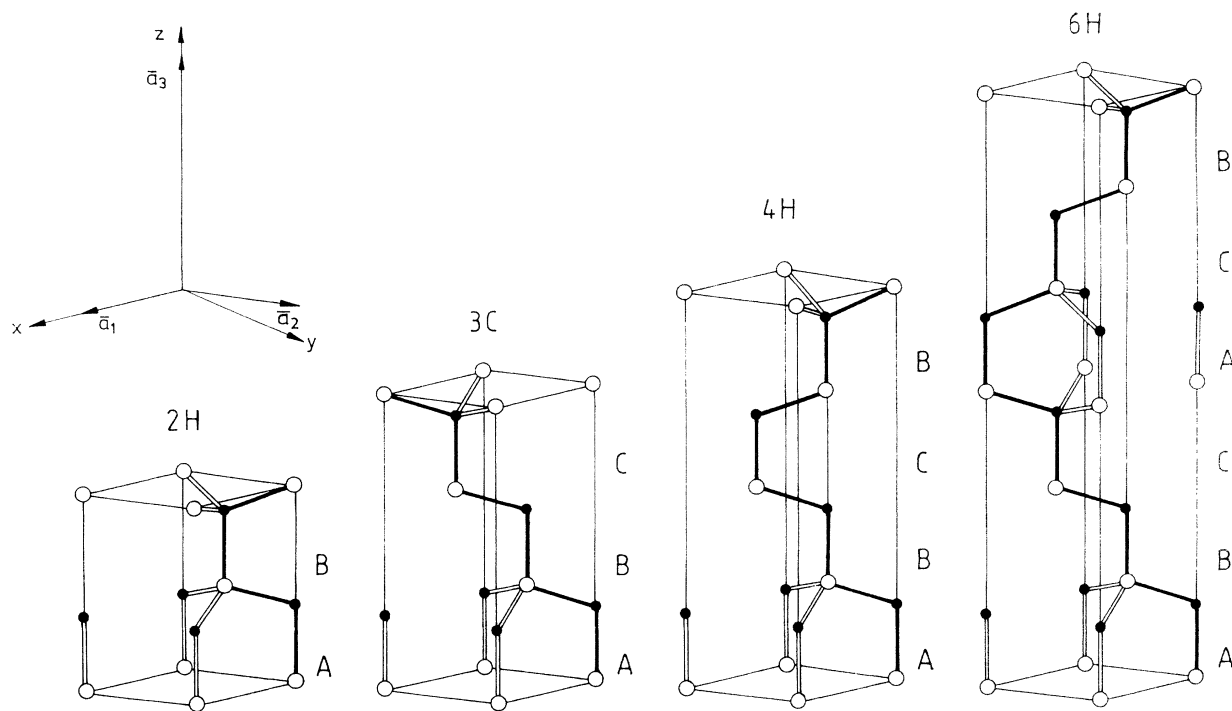


FIG. 1. Three-dimensional perspective views of the primitive hexagonal unit cells of the  $2H$ - (wurtzite)  $3C$ - (zinc blende),  $4H$ -, and  $6H$ -SiC polytypes. The characteristic chain structures of the polytypes are represented by heavy solid lines in the  $(11\bar{2}0)$  plane. The stacking sequences  $AB$  ( $2H$ ),  $ABC$  ( $3C$ ),  $ABCB$  ( $4H$ ), and  $ABCACB$  ( $6H$ ) are also indicated. The hexagonal Cartesian coordinate system as well the primitive lattice vectors are given in the upper left corner of the figure.

gin of the stacking sequences of atomic SiC double layers in  $[0001]$  direction is also indicated, following the chain links in the three different  $(11\bar{2}0)$  planes  $A$ ,  $B$ , and  $C$  in a hexagonal unit cell. In addition, the cubic ( $c$ ) or hexagonal ( $h$ ) character of the SiC double layers is given according to parallel or nonparallel limiting bonds. More strictly speaking, in  $h$  layers one of the bonds is rotated by  $180^\circ$  around the  $c$  axis. The ratio of the hexagonal layers and the total number of layers gives the percentage hexagonality of the polytype, i.e., 0% ( $3C$ ), 33% ( $6H$ ), 50% ( $4H$ ), and 100% ( $2H$ ). The indication of the double layers by  $h$  and  $c$  explains formerly usual polytype notations by Jagodzinski<sup>41</sup> and Zhdanov.<sup>42</sup> In these notations one writes  $(h)_2$  or  $\langle 1 \rangle$  for  $2H$ ,  $(hc)_2$  or  $\langle 2 \rangle$  for  $4H$ , and  $(hcc)_2$  or  $\langle 3 \rangle$  for  $6H$ .

### III. RESULTS AND DISCUSSION

#### A. Ground-state properties

A typical result of our total-energy and atomic-force calculations is represented in Fig. 3. For the wurtzite ( $2H$ ) structure we show the total-energy surface versus

the two hexagonal lattice constants  $a$  and  $c$ , more exactly the lattice constant  $a_0 = \sqrt{2}a$  and the ratio  $(c/a)$ . For a given pair  $(c,a)$  the atomic geometry is relaxed until the Hellmann-Feynman forces vanish. The total energy exhibits a pronounced minimum with respect to the ratio of the lattice constants somewhat above the ideal value of  $c/a=1.633$ . Along the "cubic" lattice constant,  $a_0 = \sqrt{2}a$ , we observe a channel in the total-energy surface. The minimum in this direction is rather flat. That means the equilibrium ratio  $c/a$  can be determined with a higher accuracy whereas the determination of the lattice constants themselves has a reduced accuracy.

Similar results are obtained for the other polytypes including  $3C$  where, however, the ideal value  $c/a=\sqrt{6}$  is kept. Therefore, close to the minimum of  $E_{\text{tot}}(c,a)$ , the surface is expected to be accurately described by the above-mentioned cubic polynomial. Explicitly, we replace the two-dimensional function  $E_{\text{tot}}(c,a)$  by the cubic form of a polynomial in  $a_0 = \sqrt{2}a$  and  $c/a$ . Typically 48 triples  $(a_0, c/a, E_{\text{tot}})$  of values are included in the least-square fit for the hexagonal polytypes. In the cubic case the ratio  $c/a = \sqrt{6}$  is fixed. We have also tested higher

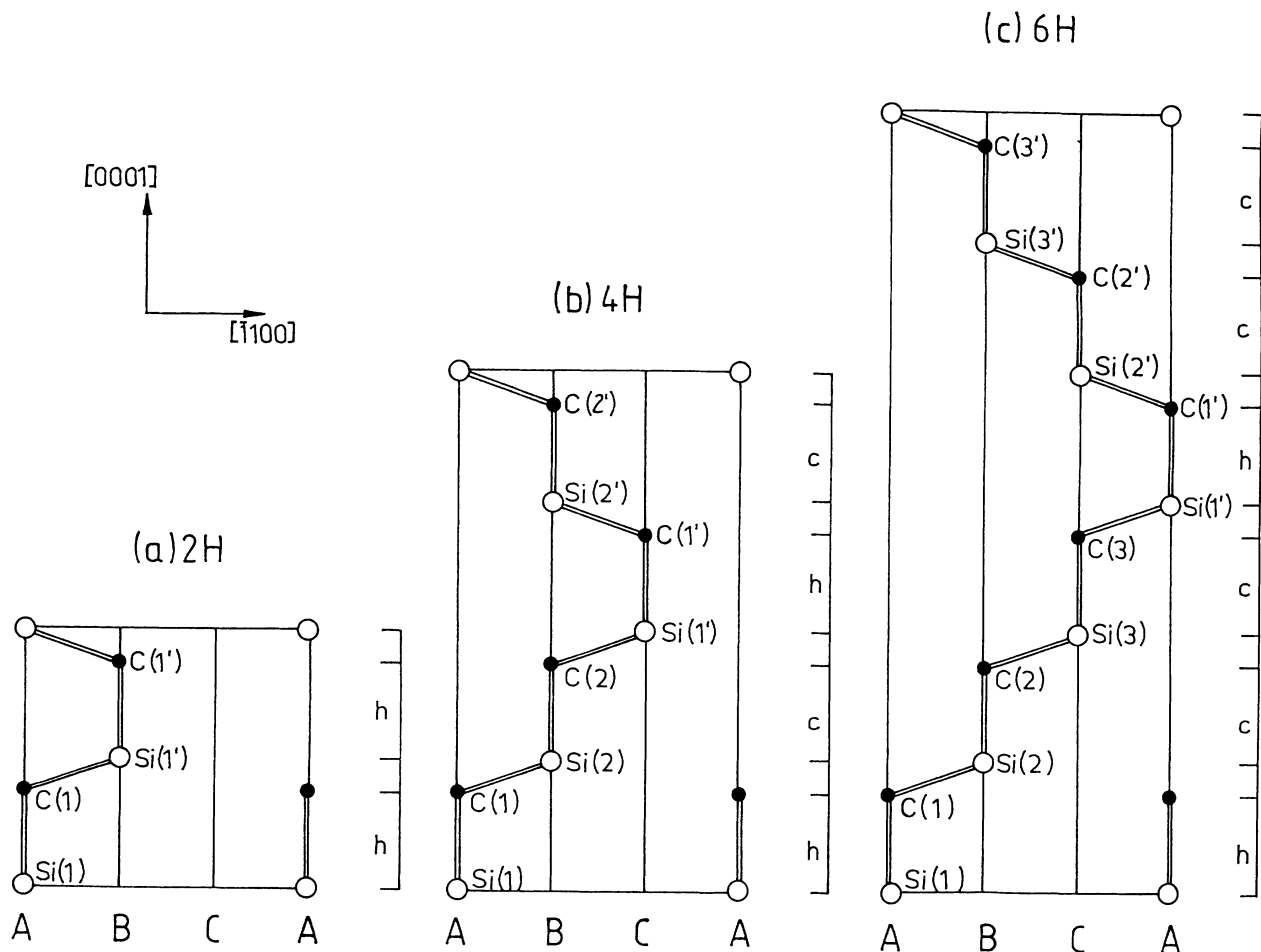


FIG. 2. The zig-zag chain structures of hexagonal SiC indicating the atomic positions. All atoms are located in the  $(11\bar{2}0)$  plane. The different  $(\bar{1}100)$  planes within the hexagonal unit cells are denoted by  $A$ ,  $B$ , and  $C$  to make obvious the staggering sequences given in Fig. 1. The cubic ( $c$ ) or hexagonal ( $h$ ) character of atomic SiC double layers in  $[0001]$  direction are given according to the parallel ( $c$ ) or nonparallel ( $h$ ) limiting bonds.

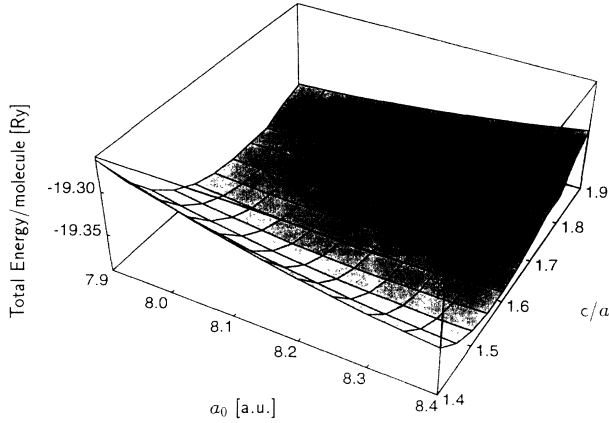


FIG. 3. Total-energy surface versus the “cubic” lattice constant  $a_0 = \sqrt{2}a$  (in atomic units) and the ratio of the hexagonal lattice constants  $c/a$ . The total energy is given in Ry per pair Si-C.

fit polynomials. However, we find that the equilibrium results can be already described with satisfying quality within the cubic approximation, at least for the collected triples around the minimum. The corresponding values resulting with and without inclusion of the atomic relaxations for the lattice constants  $c$  and  $a$ , their ratio, the volume per molecule, and the bulk modulus  $B$  are listed in Table I. The cubic form allows not only the determination of the bulk modulus as the second derivative of the total energy but also the first derivative, i.e., the hydrostatic pressure acting on the polytype when the unit-cell volume  $\Omega_0 = \frac{\sqrt{3}}{2}a^2c$  is different from the equilibrium one.

TABLE I. Calculated ground-state properties for different SiC polytypes,  $3C$  and  $pH$  ( $p = 6, 4, 2$ ). Theoretical values with (first number) or without (second number) atomic relaxations are compared with experimental data (third number).

Polytype	$a$ (Å)	$c/p$ (Å)	$c/(pa)$	$\Omega_0/p$ (Å <sup>3</sup> )	$B$ (Mbar)
$3C$	3.034	2.477	0.8165	19.754	2.22
	3.034	2.477	0.8165	19.754	2.22
	3.083 <sup>a</sup>	2.517 <sup>b</sup>	0.8165 <sup>b</sup>	20.720 <sup>a</sup>	2.24 <sup>c</sup>
$6H$	3.033	2.480	0.8177	19.753	2.18
	3.031	2.480	0.8183	19.734	2.15
	3.081 <sup>d</sup>	2.520 <sup>d</sup>	0.8179 <sup>d</sup>	20.710 <sup>d</sup>	2.234, <sup>f</sup> 2.25 <sup>g</sup>
$4H$	3.032	2.482	0.8185	19.751	2.17
	3.027	2.490	0.8226	19.760	2.11
					2.234, <sup>f</sup> 2.25 <sup>f</sup>
$2H$	3.031	2.480	0.8185	19.729	2.16
	3.020	2.506	0.8300	19.792	2.10
	3.076 <sup>e</sup>	2.524 <sup>e</sup>	0.8205 <sup>e</sup>	20.690 <sup>e</sup>	2.234, <sup>f</sup> 2.25 <sup>f</sup>

<sup>a</sup>Corresponds to Ref. 43.

<sup>b</sup>Corresponds to the deal ratio.

<sup>c</sup>Estimated from results for hexagonal SiC in Ref. 43.

<sup>d</sup>Corresponds to Ref. 5.

<sup>e</sup>Corresponds to Ref. 3.

<sup>f</sup>Corresponds to Ref. 44 and is measured for polycrystalline hexagonal SiC.

<sup>g</sup>Corresponds to Ref. 45 and is measured for polycrystalline hexagonal SiC.

Independent of the inclusion of atomic relaxations or not, the overall agreement of the theoretical values (first number: with atomic relaxations; second number: without atomic relaxations) in Table I with the experimental data (third number) is satisfactory. This holds in particular for the trend with the percentage hexagonality of the polytype. The lattice constant  $a$  perpendicular to the hexagonal axis slightly decreases with rising hexagonality. Experimentally, the reversed tendency is observed for lattice constant  $c$ . Neglecting the atomic relaxations, i.e.,  $\varepsilon(j) = \delta(j) = 0$  for the cell-internal structural parameters, i.e., taking into account nonideal tetrahedrons deformed in  $z_{\text{hex}}$  direction, we overestimate this trend remarkably. However, considering the atomic relaxations, this variation with the hexagonality can be reproduced, although it is much weaker in theory. A unique increase follows for the net quantity,  $c/(pa)$ . However, the experimental trend is overestimated (underestimated) without (with) atomic relaxations.

An extremely sensitive quantity is the volume  $\Omega_0/p$  per SiC molecule. Experimentally a tiny decrease with the hexagonality is found. This trend can be only clearly reproduced by the calculations if the atomic relaxations are included. Other theoretical studies<sup>14,15,22</sup> cannot reproduce this experimental trend because of the neglect<sup>14,22</sup> or incomplete inclusion of the internal structural degrees of freedom. Differences with the other *ab initio* pseudopotential calculations are perhaps additionally due to different details of the treatment, e.g., pseudopotentials, cutoff, and exchange-correlation functional.

When we compare not only the structural trends but also the absolute values of the lattice constants and the volume, the agreement is slightly worse. The calculated lattice constants are smaller by about 1–2%, whereas this discrepancy is somewhat larger in the case of the molecule volumes. Such discrepancies are typical for well-converged DFT-LDA calculations, since the zero-point vibrations of the atoms are neglected. Furthermore, there is a tiny temperature variation between  $T=0$  K and 300 K.<sup>43</sup> Another possible origin of the discrepancies concerns the quality of the crystals investigated in Refs. 3, 5, and 42, especially their chemical and structural perfection as well as the impurity concentration.

The bulk modulus  $B$  (cf. Table I) is rather insensitive with respect to the certain polytype structure, even if all data arise from studies of more or less hexagonal SiC, more strictly speaking from ultrasonic measurements for specimens of  $\alpha$ -SiC (Refs. 45 and 46) or reestimates for the same material.<sup>44</sup> Thereby,  $\alpha$ -SiC is usually used as a common denominator for all hexagonal and rhombohedral phases of SiC. Our theoretical data confirm this insensitivity. Nevertheless, the theory predicts a small decrease of the elastic constant with the hexagonality. In the average, we state similar discrepancies as in the case of the lattice constants. The agreement with other calculations<sup>10,11,13–18,22,23</sup> is reasonable. However, the other calculated values are somewhat smaller.

## B. Atomic relaxations

All polytypes, except the purely cubic  $3C$  structure, exhibits deviations from their associated ideal tetrahe-

drally coordinated structures, as discussed in Sec. II B. The projections on the hexagonal axis of the atomic spacings are not necessarily equal from one layer to another. The tetrahedra of nearest neighbors around every atom can be distorted along this direction, usually retaining the threefold symmetry axis parallel to the  $c$  axis.<sup>40,47</sup> In our force-minimization calculations to establish the final equilibrium geometry, this feature is evidenced by ratios  $c/(pa) \neq \sqrt{2/3}$  and nonzero parameters  $\varepsilon(j)$  and  $\delta(j)$ .

Results of the force-minimization procedure as well as a symmetrization of the coordinates according to the  $C_{6v}^4$  symmetry are represented in Fig. 4 for the cell-internal parameter  $\varepsilon$  in the wurtzite case and Table II for all hexagonal polytypes. Generally, for all pairs,  $c$  and  $a$ , the parameter  $\varepsilon$  remains small. It varies around zero indicating that already small atomic displacements parallel to the hexagonal axis make the forces vanishing. However, there is a tendency for the parameter  $\varepsilon$  to be positive. This is in agreement with the findings of other calculations<sup>48</sup> for III-V compounds with small anions. The most interesting point concerns whether the relaxation of the atomic structure is completely general or follow rules, e.g., the conservation of bond length or the conservation of bond angles. The conservation laws correspond to the relations  $\varepsilon = \frac{1}{8} \left[ \frac{8}{3} \left( \frac{a}{c} \right)^2 - 1 \right]$  or  $\varepsilon = \frac{1}{8} \left[ 1 - \sqrt{\frac{8}{3} \frac{a}{c}} \right]$  between the cell-internal parameter and the ratio of the hexagonal lattice constants. They are indicated by solid lines on the right-hand side (bond-length conservation) and the left-hand side (bond-angle conservation) in Fig. 4. For ideal ratios  $c/a = \sqrt{8/3}$  the parameter  $\varepsilon$  should vanish. This is not observed along the corresponding line in Fig. 4, indicating that the bond lengths as well as the bond angles are in general not equal in a  $2H$  structure. From Table I one observes  $c/a=1.637$ . Therefore, the cell-internal relaxation parameter should be  $\varepsilon = -0.00061$  ( $\varepsilon = 0.00031$ ) for the bond-length (bond-angle) conservation. Nevertheless, we have  $\varepsilon = 0.00080$  (cf. Table II) derived. That means, in the resulting  $2H$  structure the bond-angle conservation is more fulfilled than the bond-length conservation.

Including the atomic relaxations in  $2H$ , we find qualitatively similar results as other *ab initio* calculations,<sup>15</sup>

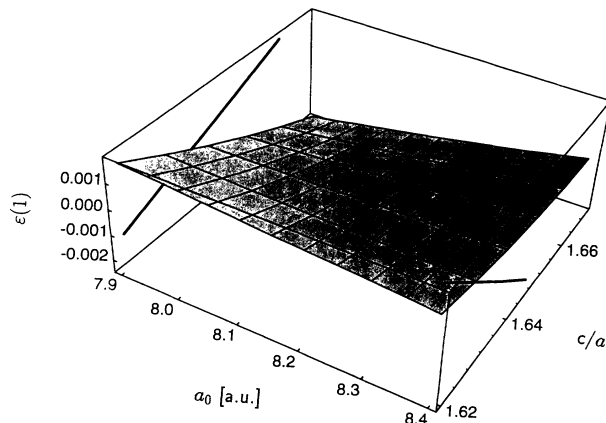


FIG. 4. Cell-internal structural parameter  $\varepsilon(1)$  of the wurtzite structure,  $2H$ -SiC, versus the two hexagonal lattice constants  $c$  and  $a$ . Results follow from force as well as total-energy-minimization procedures. The solid lines on the right-hand side (left-hand side) indicate the bond-length (bond-angle) conservation.

relaxing the structure until the isotropic stress of the zinc blende at the experimental lattice constant, and careful x-ray investigations.<sup>4</sup> The Si-C bond parallel to the  $c$ -axis is stretched in comparison to the lengths of the three other equivalent bonds of the tetrahedron. One bond length  $L(1)$  is larger than the corresponding interatomic distance in  $3C$ -SiC of  $l_{\text{ideal}}=1.858$  Å (cf. Table I). The reversed situation occurs for the other one,  $l(1)$ . The Si-C-Si bond angle is somewhat smaller than the ideal tetrahedron angle. With respect to the percentage differences our findings are also in agreement, although our values are somewhat smaller than those calculated by Cheng *et al.*<sup>15</sup> However, our geometry is more ideal than that derived by x-ray studies.<sup>4</sup>

Looking more carefully on the data of the structures giving the absolute minima in the total energy of all hexagonal polytypes  $2H$ ,  $4H$ , and  $6H$  (cf. Table II), one generally finds only small deviations from the ideal values, especially for the bond angles from the ideal tetra-

TABLE II. Geometrical parameters of hexagonal SiC polytypes from total-energy and force minimizations. Cell-internal parameters  $\varepsilon(j)$  and  $\delta(j)$ , interatomic distances  $L(j)$  and  $l(j)$  (in Å), as well as Si-C-Si bond angles  $\alpha(j)$  (in degrees) are collected for  $2H$ -,  $4H$ - and  $6H$ -SiC. In addition, the thickness  $d(j)$  (cf. Fig. 5) of a Si-C double layer (in Å) and the deformation  $\Delta(j) = 1 - l(j)/L(j)$  (in %) are given.

Polytype	$j$	$\varepsilon(j) \times 10^4$	$\delta(j) \times 10^4$	$L(j)$	$l(j)$	$\alpha(j)$	$d(j)$	$\Delta(j)$
$2H$	1	8.0	0.0	1.866	1.855	109.409	2.482 <sup>a</sup>	0.549
$4H$	1	4.8	0.0	1.866	1.855	109.321	2.480	0.625
	2	-2.3	-2.1	1.862	1.858	109.588	2.484	0.197
$6H$	1	3.7	0.0	1.865	1.856	109.351	2.480	0.506
	2	0.6	0.3	1.860	1.857	109.416	2.477	0.201
	3	-0.9	-1.2	1.860	1.858	109.536	2.485	0.127

<sup>a</sup> The value  $d(1)$  for  $2H$  is slightly larger than the value  $c/p$  in Table I. The difference, which approaches the accuracy of 0.002 Å, results from the different computational methods.  $d(1)$  results from force optimization, whereas  $c$  is determined from a polynomial fit of the total energy.

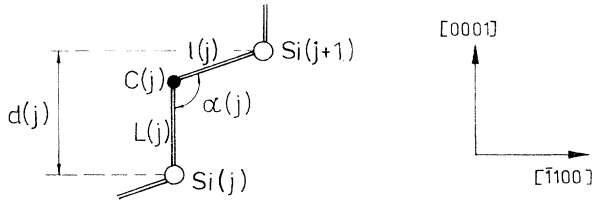


FIG. 5. One Si-C bilayer in [0001] direction and its associated geometry parameters. The same notation is used for the atoms as in Fig. 2.

hedron angle  $109.47^\circ$ . The angles vary around the ideal value by about 0.1%. Their average value approaches the ideal value.

The characteristic geometrical variables of each different double layer  $j = 1, \dots, p/2$  in the  $pH$  hexagonal structures are three: the length  $L(j)$  of the  $\text{Si}(j)\text{-C}(j)$  bond parallel to the hexagonal axis, the length  $l(j)$  of three remaining (equivalent)  $\text{C}(j)\text{-Si}(j+1)$  bonds, and the angle  $\alpha(j)$  between  $L(j)$  and  $l(j)$  as shown in Fig. 5. If there is  $j = p/2$ , the Si index  $j+1$  has to be replaced by  $j'$ . The  $3p/2$  geometrical parameters and the two lattice constants are not independent. It holds  $a = \sqrt{3}l(j) \sin(\alpha(j))$  and  $\sum_{j=1}^{p/2} [L(j) - l(j) \cos(\alpha(j))] = c/2$ . That implies that only  $(p+1)$  independent geometrical variables have to be considered, e.g.,  $a$  and  $c$  and the  $(p-1)$  cell-internal parameters as in Sec. II B.

The influence of the atomic relaxations on the bond lengths can be best seen if we look at the deviations of the tetrahedra in a bilayer from the regular form as in the zinc-blende structure. A good measure of the deformation of a coordination tetrahedron around a C atom is the quantity  $\Delta(j) = 1 - l(j)/L(j)$ , which is also listed in Table II. In agreement with a recalculation of the geometry of Cheng *et al.*<sup>15</sup> by Vignoles<sup>49</sup> we find always positive values, indicating the elongation of the hexagonal polytypes in the direction of the  $c$  axis, which is important for the growth of epitaxial layers along [0001]. The deformations  $\Delta(j)$  are more important for hexagonal layers ( $> 0.5\%$ ) than for cubic layers ( $< 0.2\%$ ). Vignoles<sup>49</sup> traced this finding back to electrostatic interactions. At short distances, steric repulsions between third neighbors in  $h$ -bilayers disfavor a conformation, but if the distance grows the electrostatic attraction has the opposite effect. The balance of the two interactions depends sensitively on the bond orientations.

Other interesting geometrical quantities are the thicknesses  $d(j)$  of the Si-C bilayers parallel to  $c$  axis. In general, they are larger than the ideal value  $2.477 \text{ \AA}$  of the  $3C$  structure. The average values give the lattice constants  $c/p$  (cf. Table I) and, therefore, also exhibit their trend with the hexagonality. In the case of  $6H$ , we observe the same sequence as careful x-ray measurements.<sup>5</sup> It holds  $d(2) < d(1), d(3)$ .

### C. Cohesive energies

In order to discuss the stability of the polytypes at low temperature, we compare the cohesive energies per

atom for the different polytypes under consideration and three different geometries in Fig. 6: We first calculate the energies of the polytypes where they are only minimized with respect to the lattice constants  $a$  and  $c$ . In a second step, the resulting structures are relaxed, i.e., the total energies are minimized not only with respect to  $a$  and  $c$  but also to the cell-internal structural parameters  $\varepsilon(j)$  and  $\delta(j)$  are determined by an atomic-force minimization. For comparison we also show the total energies for ideal tetrahedral geometries, i.e., for  $c/(pa) = \sqrt{2/3}$  and a cubic lattice constant  $a_0$  from experiment.<sup>43</sup>

Depending on the inclusion of the atomic relaxations or not we find a different energetical ordering of the polytypes and, hence, different conclusions with respect to the polytype stability. However, the underlying energetical differences are extremely small. For the remarkably deformed tetrahedra in the hexagonal structures without inclusion of atomic relaxations our calculations predict the zinc-blende structure to be stable with respect to the wurtzite one by about 8 meV/atom (cf. Fig. 6 and Table III). The zinc-blende structure seems to be also lower in energy than the other hexagonal polytypes  $6H$  and  $4H$ . However, their energy differences are smaller than 1 meV and, therefore, approach the accuracy of our calculations. Taking into account the relaxations of the cell geometries, the principal ordering of the polytypes is changed. However, the difference in the cohesive energies of the favorable  $4H$  polytype and the most unfavorable wurtzite structure approaches 3 meV/atom. Including the atomic relaxations the monotoneous trend with the percentage

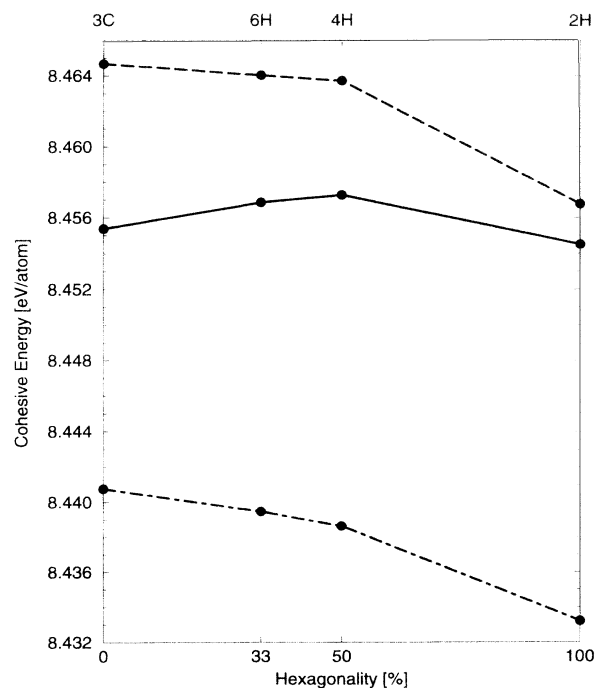


FIG. 6. The cohesive energies per atom for the  $3C$ -,  $6H$ -,  $4H$ -, and  $2H$ -SiC polytypes as obtained by *ab initio* calculations at low temperature. (a) Dashed line: unrelaxed geometries, (b) solid line: relaxed geometries, (c) dot-dashed line: ideal geometry at the experimental  $3C$  lattice constant.



TABLE III. Cohesive energies per atom (in eV) calculated in a  $12H$  unit cell for different SiC polytypes ( $3C$ ,  $6H$ ,  $4H$ ,  $2H$ ) and different geometries (a), (b), (c). (a) Unrelaxed structures (14 Monkhorst-Pack special points), (b) relaxed structures (six Chadi-Cohen special points), (c) ideal structures, i.e.,  $c/(pa) = \sqrt{2/3}$  and  $a_0 = 8.232$  a.u. from experiment for  $3C$  (Ref. 43) (14 Monkhorst-Pack special points). Due to the use of different  $k$ -point sets there is a shift between the values for the relaxed structures (b) and the two other curves.

Polytype	Unrelaxed	Relaxed	Ideal
$3C$	8.4647	8.4554	8.4408
$6H$	8.4640	8.4569	8.4395
$4H$	8.4637	8.4573	8.4386
$2H$	8.4568	8.4545	8.4332

hexagonality is destroyed. The displacement of the atoms within the unit cells, in particular, parallel to the  $c$  axis, gives rise to forces opposite to those driving the polytypism in the case of remarkably deformed tetrahedra (Fig. 6, curve  $b$ ) and ideal tetrahedra but for the experimental  $3C$  lattice constant (curve  $c$ ). Nevertheless, neglecting the difference due to the use of different  $k$ -space samplings, we conclude that the effect of relaxation on the energies is similar to that on the geometries as also observed by Cheng *et al.*<sup>15</sup> for SiC polytypes and Yeh *et al.*<sup>48</sup> for several compound semiconductors. The reduction of the energetical favoring of the zinc-blende structure is correlated with a reduction of the  $c/a$  ratio with respect to the ideal value of 0.8165. This agrees with the phenomenological correlation established by Chelikowsky and Phillips.<sup>50</sup>

External stresses due to the choice of the experimental cubic lattice constant and ideal tetrahedra seem principally to have the same influence on the polytype stability as internal stresses to the constrained atomic positions in the case (a). Figure 6 (curve  $c$ ) shows more or less the same ordering of the cohesive energies as curve  $a$ . This is somewhat in contrast to the findings of Cheng and co-workers.<sup>14,15</sup> In their (non-stress-free) structures and the stress-free and relaxed case (b) it seems to be an energetical rearrangement of the three materials  $6H$ -,  $4H$ -, and  $2H$ -SiC resulting in a favoring of the two hexagonal polytypes with low hexagonality and a shift of the  $2H$  structure towards  $3C$ . Other reasons are discrepancies in the calculational details: different C pseudopotentials, the use of the Wigner interpolation for exchange and correlation, the lower cutoff, the exact diagonalization of plane waves only until a cutoff of 10 Ry.

The absolute cohesive energies per atom listed in Table III considerably overestimate the experimental values for the  $3C$ -SiC structure of 6.34 eV.<sup>51</sup> The reason is the overestimation of such energies by the DFT-LDA mentioned

in Sec. II A. We calculate total energies per SiC molecule of about  $-19.42$  Ry for  $3C$  as well as  $2H$ -SiC. These values are very close to the total energy of  $-19.41$  Ry,<sup>11</sup> estimated from thermochemical data and atomic ionization energies. By means of the total energies  $-10.67$  Ry (C) and  $-7.50$  Ry (Si) for the free atoms one estimates differences of 8.5 eV/atom in agreement with Table III.

#### IV. SUMMARY

In conclusion, we have studied the ground-state properties of cubic and hexagonal SiC polytypes using softened *ab initio* pseudopotentials and a total-energy-minimization procedure. The results are found to be in good agreement with available experimental data. This holds especially for the structural trends versus the percentage hexagonality of the polytype, at least for the considered structures  $3C$ ,  $6H$ ,  $4H$ , and  $2H$ . We find that the atomic relaxations within the hexagonal unit cells play an important role to find the correct structural properties. Their effect on the energetics of the polytypes is of minor influence. Nevertheless, it is sufficient to influence their stability and it makes the hexagonal  $4H$  structure to the energetically most favorable one, although the different cohesive energies vary within an interval of 3 meV.

When the total energy is minimized only with respect to the hexagonal lattice constants  $a$  and  $c$  rather deformed atomic geometries are observed. Moreover, the volume per molecule increases from zinc blende to wurtzite SiC. However, after inclusion of the atomic relaxations this trend is inverted. The increase of the averaged thickness  $c/p$  per Si-C bilayer is strongly reduced resulting in a nearly constant ratio  $c/(pa)$  near the ideal value  $\sqrt{2/3}$ . Generally, the polytype geometries are closer to the ideal tetrahedron structures after relaxation.

Although the structural rearrangement of the Si and C atoms influences the polytype, it seems hardly to be of importance for the forces driving the polytypism during growth or epitaxy. The differences in the cohesive energies of different polytypes are smaller than the thermal energies at reasonable crystal-growth conditions. Hence, nonequilibrium effects related to the details of the growth and effects of the vibrating lattice are expected to be of major importance.

#### ACKNOWLEDGMENTS

The work was supported by the Sonderforschungsbereich 196 (Project No. A08) of the Deutsche Forschungsgemeinschaft and the EC Programme Human Capital and Mobility under Contract No. ERBCHRXCT 930337.

<sup>1</sup> B. Wenzien, P. Käckell, and F. Bechstedt, in *Proceedings of the 5th International Conference on Silicon Carbide and Related Materials, Washington, 1993*, edited by M. Spencer (Institute of Physics, London, 1994).

<sup>2</sup> A.R. Verma and P. Krishna, *Polymorphism and Polytypism in Crystals* (Wiley, New York, 1966).

<sup>3</sup> R.F. Adamsky and K.M. Merz, *Z. Kristallogr.* **111**, 350 (1959).

- <sup>4</sup> H. Schulz and K.H. Thiemann, *Solid State Commun.* **32**, 783 (1979).
- <sup>5</sup> A.H. Gomes de Mesquita, *Acta Crystallogr.* **23**, 610 (1967).
- <sup>6</sup> J.R. Guth and W.T. Petuskey, *J. Phys. Chem.* **91**, 5361 (1987).
- <sup>7</sup> J.S. Hartman, M.F. Richardson, B.L. Sheriff, and B.G. Winsborrow, *J. Am. Chem. Soc.* **109**, 6059 (1987).
- <sup>8</sup> D.C. Aperley *et al.*, *J. Am. Chem. Soc.* **74**, 777 (1991).
- <sup>9</sup> M. O'Keefe, *Chem. Mater.* **3**, 332 (1991).
- <sup>10</sup> N. Churcher, K. Kunc, and V. Heine, *Solid State Commun.* **56**, 177 (1985).
- <sup>11</sup> P.J.H. Denteneer and W. van Haeringen, *Phys. Rev. B* **33**, 2831 (1986).
- <sup>12</sup> P.E. Van Camp, V.E. Van Doren, and J.T. Devreese, *Phys. Status Solidi B* **146**, 573 (1988).
- <sup>13</sup> K.J. Chang and M.L. Cohen, *Phys. Rev. B* **35**, 8196 (1987).
- <sup>14</sup> C. Cheng, R.J. Needs, V. Heine, and N. Churcher, *Europhys. Lett.* **3**, 475 (1987); C. Cheng, R.J. Needs, and V. Heine, *J. Phys. C* **21**, 1049 (1988).
- <sup>15</sup> C. Cheng, V. Heine, and R.J. Needs, *J. Phys. Condens. Matter* **2**, 5115 (1990).
- <sup>16</sup> B.H. Cheong, K.H. Chang, and M.L. Cohen, *Phys. Rev. B* **44**, 1053 (1991).
- <sup>17</sup> B. Wenzien, P. Käckell, and F. Bechstedt, *Surf. Sci.* **307-309**, 989 (1994); cf. Ref. 1.
- <sup>18</sup> P.J.H. Denteneer and W. van Haeringen, *Solid State Commun.* **65**, 115 (1988).
- <sup>19</sup> C. Cheng, V. Heine, and I.L. Jones, *J. Phys. Condens. Matter* **2**, 5097 (1990).
- <sup>20</sup> P. Hohenberg and W. Kohn, *Phys. Rev.* **136**, B864 (1964).
- <sup>21</sup> W. Kohn and L.J. Sham, *Phys. Rev.* **140**, A1133 (1965).
- <sup>22</sup> W.R.L. Lambrecht, B. Segall, M. Methfessel, and M. van Schilfgaarde, *Phys. Rev. B* **44**, 3685 (1991).
- <sup>23</sup> W.R.L. Lambrecht and B. Segall, in *Wide Band-Gap Semiconductors*, edited by T.D. Moustakas, J.I. Pankove, and Y. Hamakawa, MRS Symposia Proceedings No. 242 (Materials Research Society, Pittsburgh, 1992), p. 367.
- <sup>24</sup> H. Hellmann, *Einführung in die Quantenchemie* (Deuticke, Leipzig, 1937).
- <sup>25</sup> R.P. Feynman, *Phys. Rev.* **56**, 340 (1939).
- <sup>26</sup> D.M. Ceperley and B.I. Alder, *Phys. Rev. Lett.* **45**, 566 (1980).
- <sup>27</sup> P. Perdew and A. Zunger, *Phys. Rev. B* **23**, 5048 (1981).
- <sup>28</sup> G.B. Bachelet, D.R. Hamann, and M. Schlüter, *Phys. Rev. B* **26**, 4199 (1982).
- <sup>29</sup> L. Kleinman and D.M. Bylander, *Phys. Rev. Lett.* **48**, 1425 (1982).
- <sup>30</sup> R. Stumpf, X. Gonze, and M. Scheffler (unpublished); X. Gonze, R. Stumpf, and M. Scheffler, *Phys. Rev. B* **44**, 8503 (1991).
- <sup>31</sup> P.J.H. Denteneer, C.G. Van de Walle, and S.T. Pantelides, *Phys. Rev. B* **39**, 10 809 (1989).
- <sup>32</sup> P. Käckell and F. Bechstedt (unpublished).
- <sup>33</sup> R. Car and M. Parrinello, *Phys. Rev. Lett.* **55**, 2471 (1985).
- <sup>34</sup> R. Stumpf and M. Scheffler, *Comput. Phys. Commun.* **79**, 447 (1994).
- <sup>35</sup> F.D. Murnaghan, *Proc. Natl. Acad. Sci. U.S.A.* **30**, 244 (1944).
- <sup>36</sup> B. Farid and R.J. Needs, *Phys. Rev. B* **45**, 1067 (1992).
- <sup>37</sup> H.J. Monkhorst and J.D. Pack, *Phys. Rev. B* **13**, 5188 (1976).
- <sup>38</sup> D.J. Chadi and M.L. Cohen, *Phys. Rev. B* **8**, 5747 (1973).
- <sup>39</sup> R.A. Evarestov and V.P. Smirnov, *Phys. Status Solidi B* **119**, 9 (1983).
- <sup>40</sup> R.W.G. Wyckhoff, *Crystal Structures* (Interscience Publishers, New York, 1964), Vol. 1.
- <sup>41</sup> H. Jagodzinski, *Acta Crystallogr.* **2**, 201 (1949); **7**, 300 (1954).
- <sup>42</sup> G.S. Zhdanov, *C. R. Acad. Sci. USSR* **48**, 43 (1945).
- <sup>43</sup> A. Taylor and R.M. Jones, in *Silicon Carbide—A High-Temperature Semiconductor*, Proceedings of the Conference on Silicon Carbide, Boston, 1959, edited by J.R. O'Connor and J. Smiltens (Pergamon Press, New York, 1960), p. 147.
- <sup>44</sup> D.H. Yean and J.R. Ritter, *J. Phys. Chem. Solids* **32**, 653 (1971).
- <sup>45</sup> E. Schreiber and N. Soga, *J. Am. Ceram. Soc.* **49**, 342 (1966).
- <sup>46</sup> R.D. Carnahan, *J. Am. Ceram. Soc.* **51**, 223 (1968).
- <sup>47</sup> W. Weltner, Jr., *J. Chem. Phys.* **51**, 2469 (1969).
- <sup>48</sup> C.-Y. Yeh, Z.W. Lu, S. Froyen, and A. Zunger, *Phys. Rev. B* **46**, 10 086 (1993).
- <sup>49</sup> G.L. Vignoles, *J. Cryst. Growth* **118**, 430 (1992).
- <sup>50</sup> J.R. Chelikowsky and J.C. Phillips, *Phys. Rev. B* **17**, 2453 (1978).
- <sup>51</sup> W.A. Harrison, *Electronic Structure and the Properties of Solids* (Dover, New York, 1989).

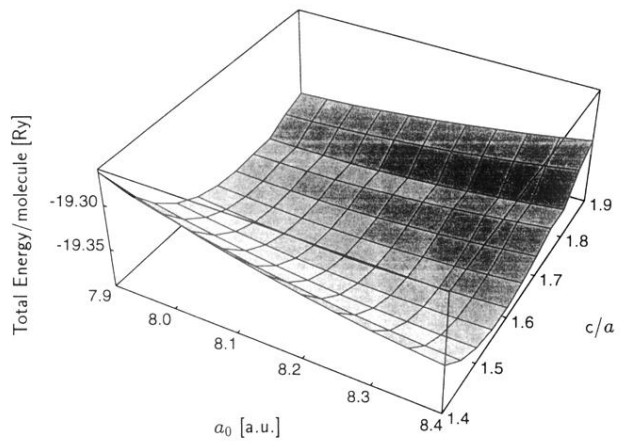


FIG. 3. Total-energy surface versus the “cubic” lattice constant  $a_0 = \sqrt{2}a$  (in atomic units) and the ratio of the hexagonal lattice constants  $c/a$ . The total energy is given in Ry per pair Si-C.

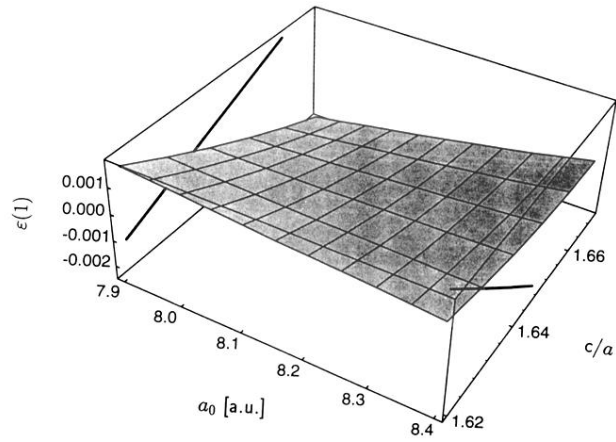


FIG. 4. Cell-internal structural parameter  $\varepsilon(1)$  of the wurtzite structure,  $2H$ -SiC, versus the two hexagonal lattice constants  $c$  and  $a$ . Results follow from force as well as total-energy-minimization procedures. The solid lines on the right-hand side (left-hand side) indicate the bond-length (bond-angle) conservation.